

# **Advanced CLARITY Methods for Rapid and High-Resolution Imaging of Intact Tissues**

Raju Tomer, PhD, and Karl Deisseroth, PhD

---

Department of Bioengineering  
Department of Psychiatry and Behavioral Sciences  
CNC Program, Howard Hughes Medical Institute  
Stanford University  
Stanford, California



## Introduction

CLARITY is a method for chemical transformation of intact biological tissues into a hydrogel-tissue hybrid, which becomes amenable to interrogation with light and macromolecular labels while retaining fine structure and native biological molecules. This emerging accessibility of information from large intact samples has created both new opportunities and new challenges. In this chapter, we describe next-generation methods spanning multiple dimensions of the CLARITY workflow. These methods range from a novel approach to simple, reliable, and efficient lipid removal without electrophoretic instrumentation (passive CLARITY), to optimized objectives and integration with light-sheet optics (CLARITY-optimized light-sheet microscopy, or COLM) for accelerating data collection from clarified samples by several orders of magnitude while maintaining or increasing quality and resolution. These methods may find application in the structural and molecular analysis of large assembled biological systems such as the intact mammalian brain.

One goal of modern neuroscience is to map the architecture of neural circuits with both high (wiring-level) resolution and broad (brainwide) perspective. This challenge has drawn the attention of generations of scientists, beginning with Ramón Y Cajal's detailed representations of neurons visualized at high resolution with the Golgi staining technique while embedded within semi-intact brain tissue (Ramón Y Cajal, 1904). Principles fundamental to the understanding of neural systems can result from such an integrative approach, but although progress has been made, many challenges and opportunities remain.

Over the last few decades, electron microscopy (EM) has emerged as a foundational method for deciphering details of neuronal circuit structure (Bock et al., 2011; Briggman et al., 2011; Kim et al., 2014). The key advantage of EM in this regard (relative to light microscopy) is the identification of presynaptic active zones containing neurotransmitter vesicles apposed to postsynaptic structures. In addition, EM facilitates visualization of some of the very finest branches of axons. However, EM tissue mapping requires relatively slow steps involving ultrathin sectioning/ablation and reconstruction; most importantly, the sample contrast preparation is largely incompatible with rich molecular phenotyping that could provide critical information on cell and synapse type. Ideally, datasets resulting from intact-brain mapping should be linkable to molecular information on the types of cells and synapses that are imaged structurally, and even to dynamical information on natural activity pattern history (in these same circuits) known to be

causally relevant to animal behavior. Suitable light-based imaging approaches, combined with specific genetic or histochemical molecular labeling methods, have emerged as important tools for visualizing the structural, molecular, and functional architecture of biological tissues, with a particularly vital role to play in emerging brainwide, high-resolution neuroanatomy.

Confocal methods revolutionized light microscopy by enabling optical sectioning in thick (tens of micrometers) fluorescently labeled samples, thereby allowing three-dimensional (3D) reconstruction without the need for ultrathin physical sectioning. (Conchello and Lichtman, 2005). Two-photon microscopy further increased the accessible imaging depth (to hundreds of micrometers) even in living tissue samples (Helmchen and Denk, 2005), and adaptive-optics approaches have improved imaging depth further (Tang et al., 2012). However, light microscopy remains limited for imaging throughout intact vertebrate nervous systems. (For example, mouse brains span many millimeters even in the shortest spatial dimension, and are opaque on this scale owing chiefly to light scattering.)

As a step in this direction, new methods have emerged to increase tissue transparency (Dodt et al., 2007; Hama et al., 2011; Ke et al., 2013) by chemically reducing the scattering of light traveling through the tissue sample. Although intriguing and effective, these approaches are not generally suitable for detailed molecular phenotyping, since most tissues (e.g., the intact mature brain) remain largely impenetrable to macromolecular antibody or oligonucleotide labels. These limitations motivated the recent development of CLARITY (Chung et al., 2013; Tomer et al., 2014), which involves the removal of lipids in a stable hydrophilic chemical environment to achieve transparency of intact tissue, preservation of ultrastructure and fluorescence, and accessibility of native biomolecular content to antibody and nucleic acid probes.

## Clarifying Large Tissue Volumes

CLARITY builds on chemical principles to grow hydrogel polymers from inside the tissue in order to provide a support framework for structural and biomolecular content (Fig. 1). This is achieved first by infusing a cold (4°C) cocktail of hydrogel monomers (for example, acrylamide with bisacrylamide), formaldehyde, and thermally triggered initiators into the tissue, followed by polymerization of the hydrogel at 37°C. Formaldehyde serves the dual purposes of cross-linking amine-containing tissue components to each other, as well as covalently binding the hydrogel monomers to these native biomolecules, which include

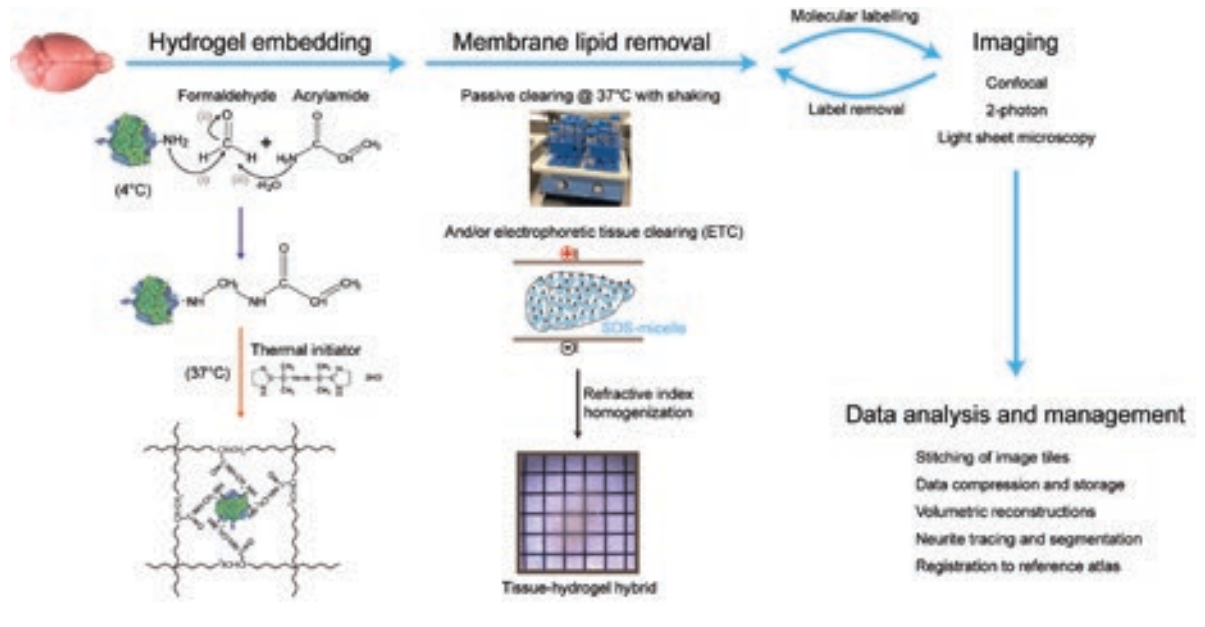


**Figure 1.** CLARITY pipeline overview. The tissue sample, e.g., an intact mouse brain, is perfused with cold hydrogel monomer solution that contains a cocktail of acrylamide, bisacrylamide, formaldehyde, and thermal initiator. Formaldehyde mediates cross-linking of biomolecules to acrylamide monomers via amine groups; presumptive chemistry of this process is shown. Hydrogel polymerization is initiated by incubating the perfused tissue at 37°C, resulting in a meshwork of fibers that preserves biomolecules and structural integrity of the tissue. Lipid membranes are removed by passive thermal clearing in SBC solution at 37°C or by electrophoretic tissue clearing (ETC). The resulting intact tissue–hydrogel hybrid can undergo multiple rounds of molecular and structural interrogation using immunohistochemistry and light microscopy. A dedicated computational infrastructure is needed to analyze and store the data. All animal experiments were carried out with Stanford University institutional review board approval.

proteins, nucleic acids, and other small molecules (Fig. 1), but not the vast majority of cellular membrane phospholipids. After the hydrogel polymerization is triggered, lipids (responsible for preventing access of both photons and molecular labels to deep structures) can then be readily removed without destroying or losing native tissue components using strong ionic detergent-based clearing solution (borate-buffered 4% sodium-dodecyl-sulfate) at 37°C, either passively with gentle recirculation or with active electrophoretic forcing (the latter greatly accelerates clearing but introduces some experimental complexity and risk). The resulting lipid-extracted and structurally stable tissue–hydrogel hybrid is immersed in a refractive index (RI) homogenization solution (e.g., 87% glycerol or FocusClear; RI ~1.454) to render the intact brain transparent to light. By allowing multiple rounds of histochemical labeling and elution in the same tissue, CLARITY provides unusually rich access to molecular and structural information.

### Imaging Large Clarified Tissue Volumes

The next major challenge after achieving access to clarified large tissues is to develop optimized and high-resolution deep-imaging approaches. One of the

most important components of any light microscopy system is the detection objective (Fig. 2a), which sets the resolution that can be achieved and the maximum sample size that can be imaged. We have accordingly advised objective manufacturers to facilitate development for CLARITY samples, and these new objectives are becoming available.

In addition to optimized detection optics, the nature of the microscopy system is important for achieving high imaging speed and minimizing photo-bleaching. While confocal and two-photon microscopes have been the workhorse systems in volumetric imaging for the reasons described above, over the past 20 years, light-sheet fluorescence microscopy has emerged as a powerful approach for high-speed volumetric imaging. Figure 2b compares the mechanistic foundations of these three imaging modalities. Confocal and two-photon are point-scanning techniques, detecting optical signals point by point to construct an image. Light-sheet microscopy, in contrast, builds on a hundred-year-old idea to illuminate the sample from the side with a thin sheet of light, and detect the emitted fluorescence signal with an in-focus, orthogonally arranged objective (Siedentopf and Zsigmondy, 1903; Huiskens and Stainier, 2009). The optical sectioning

is achieved by confining illumination to a selective plane, which enables the use of fast charge-coupled device (CCD) or scientific complementary metal-oxide semiconductor (sCMOS) cameras to capture the whole image simultaneously, and results in an increase of 2–3 orders of magnitude in imaging speed

compared with confocal and two-photon microscopy. Moreover, light-sheet microscopy minimizes photo-bleaching (Fig. 2b) by confining illumination to the plane of interest. Taken together, these properties of light-sheet microscopy may be well suited for imaging large clarified samples.

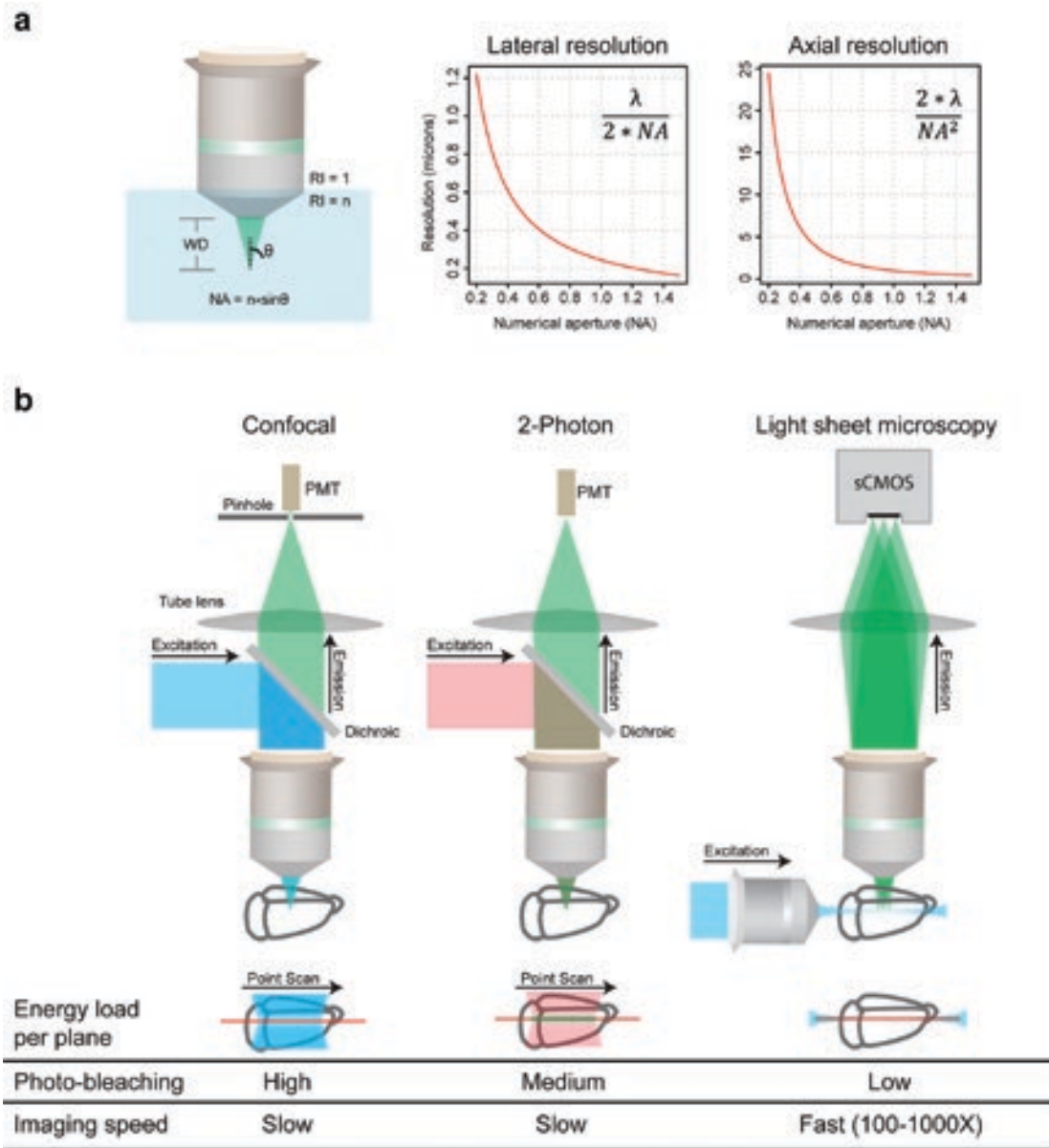


**Figure 2.** Imaging clarified samples. **a**, Key microscope objective parameters relevant to CLARITY are WD, NA, RI ( $n$ ), and multicolor correction. WD is the distance between the objective lens and the focal plane. NA relates to the fraction of total emitted signal collected by an objective, and higher NA enables higher resolution. The graphs plot diffraction-limited lateral and axial resolution parameters as a function of NA, assuming  $\lambda = 500$  nm. **b**, Comparison of confocal, two-photon, and light-sheet microscopy. Confocal microscopy achieves optical sectioning by employing a pinhole in front of the photomultiplier tubes (PMTs). Two-photon microscopy utilizes the fact that only simultaneous absorption of two photons (of longer wavelengths) results in fluorescence signal emission, an event more likely to occur at the point of highest light intensity in the sample, i.e., the focal plane. Light-sheet fluorescence microscopy achieves optical sectioning by selectively confining the illumination to the plane of interest. Confocal and two-photon microscopy use point scanning and hence are inherently slow, whereas light-sheet microscopy uses fast sCMOS/CCD cameras to image the selectively illuminated focal plane, resulting in 2–3 orders of magnitude faster imaging speed and minimal photo-bleaching.

## NOTES

**CLARITY-optimized light-sheet microscopy**

A light-sheet microscope consists of a standard wide-field detection optical arm, which includes the detection objective, the tube lens, and a camera, and the orthogonally arranged, independent illumination arm consisting of a low-numerical aperture (NA) objective, tube lens, and either a cylindrical lens to generate a static light sheet or galvanometer-scanners/ $f$ -theta lens for creating dynamic light sheets with a Gaussian or Bessel beams (Weber and Huisken, 2011). Conventional light-sheet microscopy suffers from image quality degradation due to out-of-focus scattered light. Thus, several methods have been developed to help reject out-of-focus light in light-sheet microscopy (at some cost in imaging speed, increased photo-bleaching, and instrumentation complexity), such as structured illumination.

We developed CLARITY-optimized light-sheet microscopy (COLM) to maximize the compatibility of clarified samples with light-sheet microscopy, using CLARITY objectives (25 $\times$  and 10 $\times$ , Olympus), a fast sCMOS camera, two-axis galvanometer scanners along with the  $f$ -theta lens, a low-NA objective to generate dynamic light sheets using a Gaussian beam, an optically homogeneous sample manipulation system (see below, Sample mounting apparatus for COLM), and an xyz-theta sample mount stage that provides a long travel range of 45 mm in each dimension to enable imaging of large samples (Fig. 3). COLM employs synchronized illumination detection to improve imaging quality, especially at higher depths (Fig. 3c), exploiting the unidirectional (as opposed to standard bidirectional) readout mode available in next-generation sCMOS cameras. The scanning beam (which creates the dynamic light sheet) is synchronized with the unidirectional single-line readout of the emitted signal, resulting in a virtual slit arrangement that rejects out-of-focal-plane signal caused by scattering deeper in the sample. Automated-alignment parameter calibration (using linear adaptation) in COLM corrects for misalignment artifacts across the whole sample space (Fig. 3d).

**Sample mounting apparatus for COLM**

The final component of COLM is a CLARITY-optimized sample mounting strategy that minimizes optical inhomogeneity along the detection path (Fig. 3b). Clarified whole mouse brain (or any large clarified intact tissue, such as a spinal cord) is mounted in a cuvette made of fused quartz glass (standard cuvettes used for spectrophotometer measurements) filled with FocusClear; note that the RI of fused quartz ( $\sim 1.458$ ) is nearly identical to that of FocusClear.

Using a bottom adapter (Fig. 3b), the sample cuvette is mounted onto the xyz-theta stage, inside the sample chamber (Fig. 3b). The much larger chamber is then filled with a relatively economically priced custom RI matching liquid (RI 1.454), resulting in an optically homogeneous sample manipulation system.

Figure 3b compares the images taken using standard light-sheet microscopy or COLM. We performed imaging of whole-brain samples using 10 $\times$  or 25 $\times$  magnification objectives (Figs. 4, 5).

**Discussion**

CLARITY allows molecular and structural interrogation of tissue by allowing deep imaging of transgenic and/or biochemically labeled tissue samples. To achieve the best imaging quality, careful preparation of the sample and optical setup is crucial. First, as demonstrated in Figure 2, key relevant properties of the objective must be considered, including NA, working distance (WD), color correction, and RI correction. We explored the emerging commercially available and custom solutions, and found that it is indeed possible to achieve deep high-resolution and overall high-quality imaging in clarified samples (Figs. 4, 5). Other water immersion, oil immersion, or air objectives may also prove useful for quality imaging deep in tissue.

The major limitations of confocal and two-photon microscopes are as follows: (1) slow speed owing to point scanning mechanisms (Fig. 2) and (2) damage to tissues and fluorophores caused by redundant illumination of the whole sample for every optical plane imaged, limiting the sample size that can be imaged in a reasonable timeframe before the sample is completely photo-bleached (particularly in the case of confocal microscopy). Light-sheet microscopy now emerges as an alternative for fast 3D imaging of large clarified samples, as described above.

We assessed the compatibility of clarified samples with light-sheet microscopy, observing 2–3 orders of magnitude faster imaging speed with minimal photo-bleaching. For example, it was possible to image an entire mouse brain in  $\sim 4$  h using a 10 $\times$  magnification objective and in  $\sim 1.5$  d using a 25 $\times$  objective, as opposed to many days and months, respectively, with a confocal microscope. COLM is especially well suited for interrogation of large tissue samples labeled with transgenic or histochemical techniques. The increased speed of acquisition and higher quality of data generated via CLARITY using new microscopy methods, combined with high-speed CLARITY processing itself enabled by parallelized and efficient

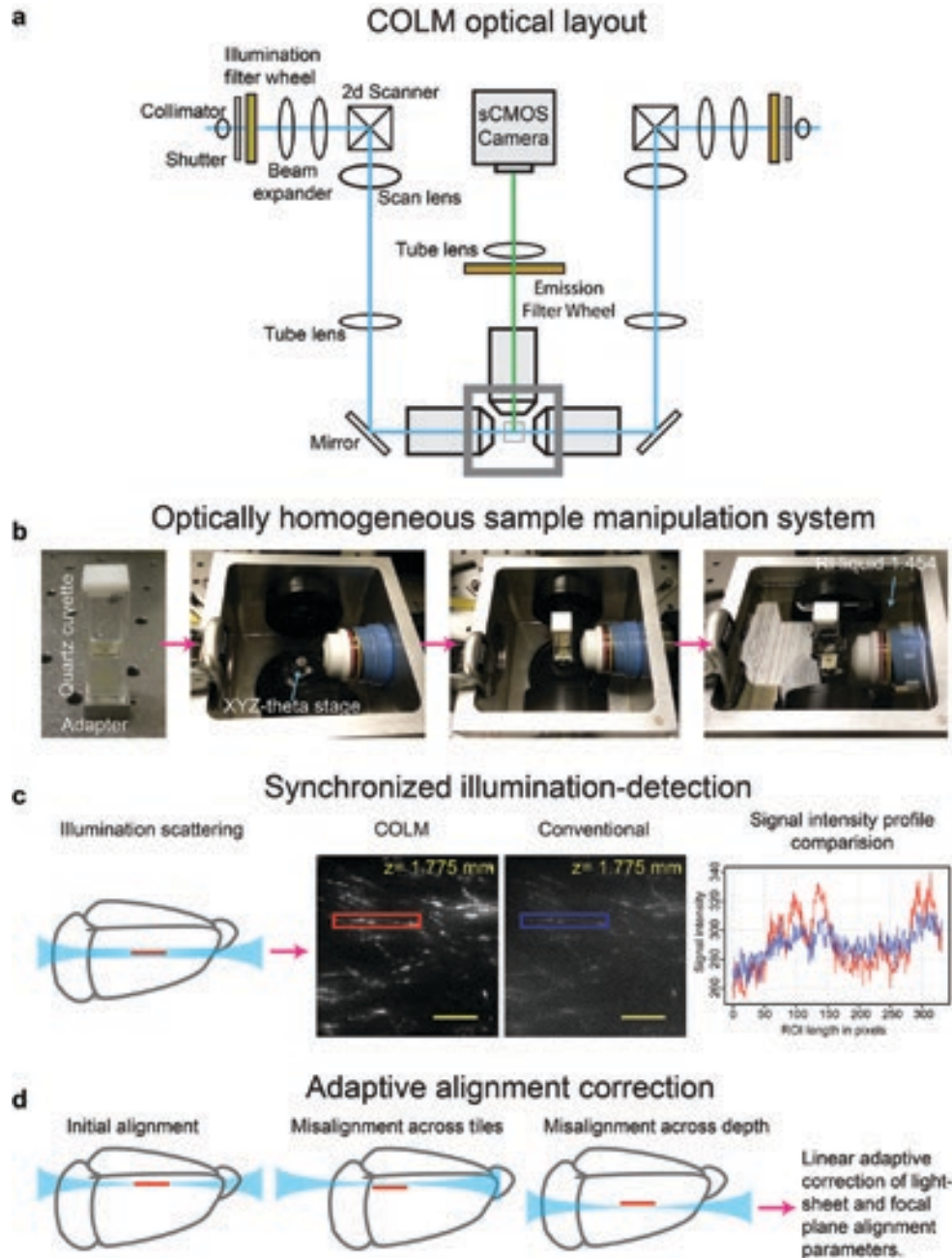


**Figure 3.** COLM for large intact samples. **a**, Optical layout of the COLM microscope. Two light sheets are created from opposite sides; shown are galvanometer scanners, scan lens, tube lens, and illumination objectives. The emitted fluorescence is imaged with an in-focus detection objective, tube lens, and sCMOS camera. Illumination and emission filter wheels (motorized) are used to generate well-defined excitation light and emission signal bands, respectively. The innovations required for COLM are discussed in **b–d**, and the schematic is shown in Supplemental Figure 2 (<http://clarityresourcecenter.com/COLM.html>). **b**, Optically homogeneous sample mounting framework for large intact samples. Clarified samples, such as intact adult mouse brain, are mounted in a quartz cuvette filled with RI matching solution such as FocusClear. Note that the RI of quartz glass (~1.458) is nearly identical to that of FocusClear (~1.454). A bottom adapter is used to attach the cuvette to the xyz-theta stage in the sample chamber, which is then filled with a matching RI liquid (~1.454). This results in an optically homogeneous sample manipulation system with minimal RI transition boundaries. **c**, Synchronized illumination and detection are achieved by synchronizing the scanning beam with the unidirectional readout of a sCMOS camera chip, resulting in a virtual-slit effect that enables substantially improved imaging quality, as illustrated by the images shown acquired from the same plane with COLM and with conventional light-sheet microscopy. The graph at right compares the signal intensity profile of a field acquired with COLM (red) with one acquired by conventional light-sheet microscopy (blue). **d**, Large clarified samples can have significant RI inhomogeneity, resulting in the need for correction of misalignment of illumination with the focal plane of the detection objective. We achieved this with a linear adaptive calibration procedure before starting the imaging experiment. Scale bars, **a–d**, 100  $\mu\text{m}$ .

## NOTES

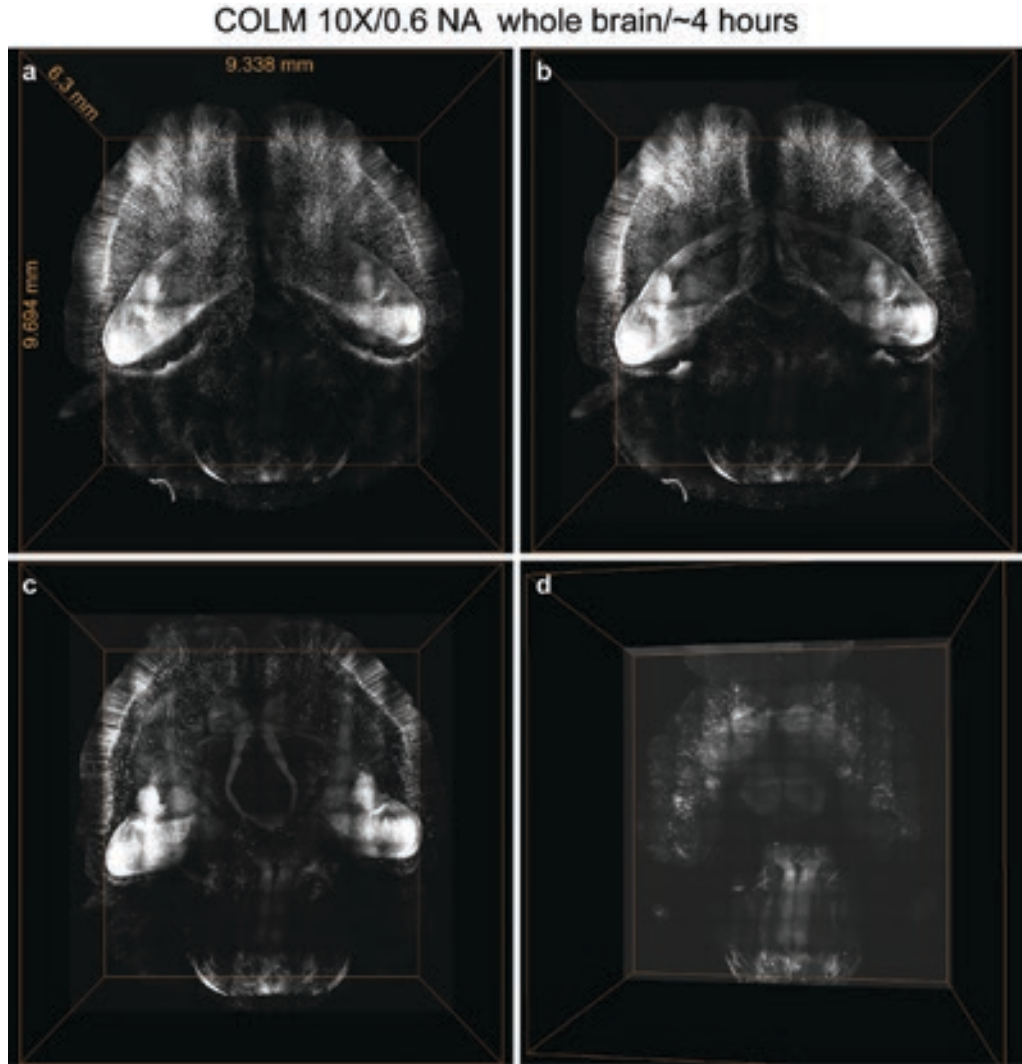


**Figure 4.** Ultrafast imaging of whole mouse brain using COLM. *a*, Volume rendering of whole mouse brain dataset acquired from an intact clarified *Thy1*-EYFP mouse brain using COLM. *b*, *c*, and *d* illustrate internal details of the intact mouse brain volume visualized by successive removal of occluding dorsal-side images. The brain was perfused with 0.5% (wt/vol) acrylamide monomer solution and clarified passively at 37°C with gentle shaking. Camera exposure time of 20 ms was used, and the RI liquid 1.454 was used as immersion media. The entire dataset was acquired in ~4 h using a 10×, 0.6 NA objective.

tissue transformation protocols described here, together define a versatile and efficient platform for structural and molecular interrogation of large and fully assembled tissues.

### Acknowledgments

We thank the entire Deisseroth Lab for helpful discussions, Anna Lei for technical assistance, and Li Ye and Brian Hseuh for help with sample preparations. All CLARITY tools and methods described are distributed and supported

freely (clarityresourcecenter.org, <http://wiki.claritytechniques.org>) and discussed in an open forum ([forum.claritytechniques.org](http://forum.claritytechniques.org)).

This chapter is excerpted from a previously published article in *Nature Protocols* 2014;9(7):1682–1697. All materials from the original article, including figures and videos, along with supplementary materials, are available in high resolution at <http://clarityresourcecenter.com/COLM.html>.

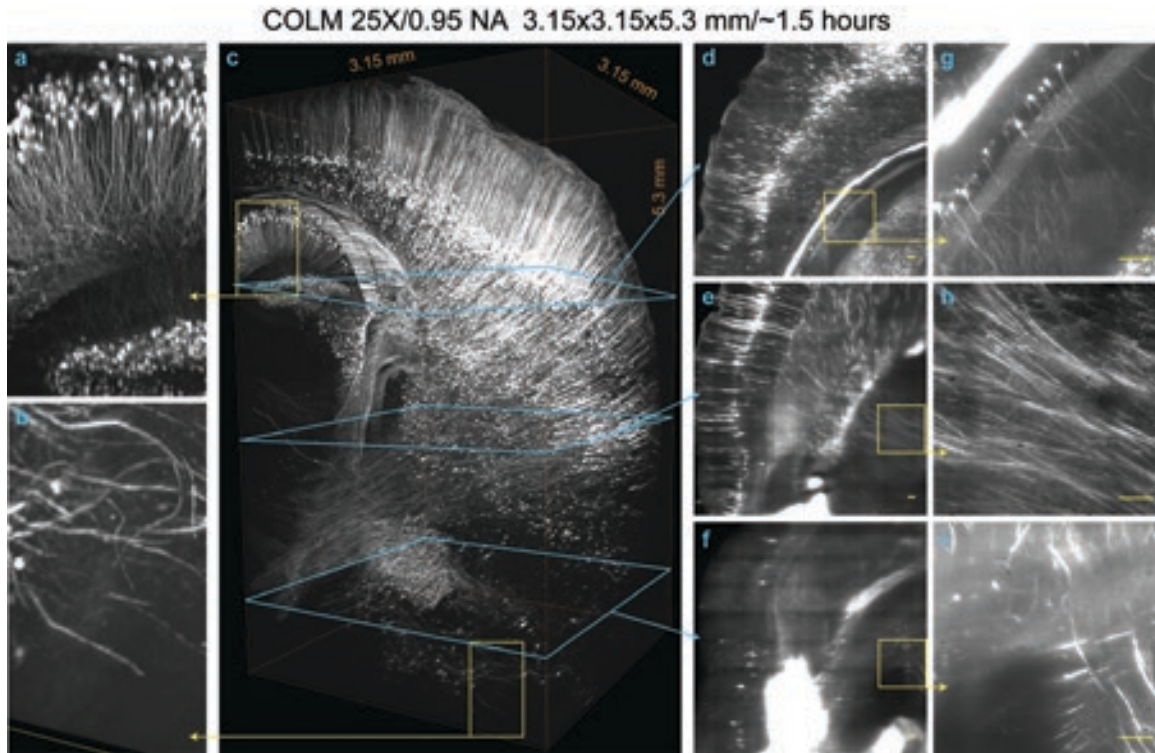


**Figure 5.** Fast high-resolution imaging of clarified brain using COLM.  $3.15 \times 3.15 \times 5.3$  mm volume acquired from an intact clarified *Thy1*-EYFP mouse brain using COLM with 25 $\times$  magnification; the brain had been perfused with 0.5% (wt/vol) acrylamide monomer solution. The complete image dataset was acquired in  $\sim 1.5$  h; for optimal contrast, the lookup table (LUT) of zoomed-in images was linearly adjusted between panels. *a* and *b* show magnified views from panel *c* regions defined by yellow squares. *d–i* show maximum-intensity projections over a 50  $\mu$ m thick volume, as shown by the progression of cyan and yellow boxes and arrows. Camera exposure time of 20 ms was used; RI liquid 1.454 was used as the immersion medium. Scale bars, *a–d*, 100  $\mu$ m.

## References

- Bock DD, Lee WC, Kerlin AM, Andermann ML, Hood G, Wetzell AW, Yurgenson S, Soucy ER, Kim HS, Reid RC (2011) Network anatomy and *in vivo* physiology of visual cortical neurons. *Nature* 471:177–182.
- Briggman KL, Helmstaedter M, Denk W (2011) Wiring specificity in the direction-selectivity circuit of the retina. *Nature* 471:183–188.
- Chung K, Wallace J, Kim SY, Kalyanasundaram S, Andalman AS, Davidson TJ, Mirzabekov JJ, Zalocusky KA, Mattis J, Denisin AK, Pak S, Bernstein H, Ramakrishnan C, Grosenick L, Gradinaru V, Deisseroth K (2013) Structural and molecular interrogation of intact biological systems. *Nature* 497:332–337.
- Conchello JA, Lichtman JW (2005) Optical sectioning microscopy. *Nat Methods* 2:920–931.
- Dotd HU, Leischner U, Schierloh A, Jahrling N, Mauch CP, Deininger K, Deussing JM, Eder M, Zieglgansberger W, Becker K (2007) Ultramicroscopy: three-dimensional visualization of neuronal networks in the whole mouse brain. *Nat Methods* 4:331–336.
- Hama H, Kurokawa H, Kawano H, Ando R, Shimogori T, Noda H, Fukami K, Sakaue-Sawano A, Miyawaki A (2011) Scale: a chemical approach for fluorescence imaging and reconstruction of transparent mouse brain. *Nat Neurosci* 14:1481–1488.
- Helmchen F, Denk W (2005) Deep tissue two-photon microscopy. *Nat Methods* 2:932–940.
- Huisken J, Stainier DY (2009) Selective plane illumination microscopy techniques in developmental biology. *Development* 136:1963–1975.
- Ke MT, Fujimoto S, Imai T (2013) SeeDB: a simple and morphology-preserving optical clearing agent for neuronal circuit reconstruction. *Nat Neurosci* 16:1154–1161.

## NOTES

- Kim JS, Greene MJ, Zlateski A, Lee K, Richardson M, Turaga SC, Purcaro M, Balkam M, Robinson A, Behabadi BF, Campos M, Denk W, Seung HS, EyeWriters (2014) Space-time wiring specificity supports direction selectivity in the retina. *Nature* 509:331–336.
- Kim SY, Chung K, Deisseroth K (2013) Light microscopy mapping of connections in the intact brain. *Trends Cogn Sci* 17:596–599.
- Ramón Y Cajal S (1904) *Textura del sistema nervioso del hombre y de los vertebrados*. Vol 2. Nicholas Moya.
- Siedentopf H, Zsigmondy R (1903) Über Sichtbarmachung und Größenbestimmung ultramikroskopischer Teilchen, mit besonderer Anwendung auf Goldrubingläser. *Annalen der Physik* 10:1–39.
- Tang J, Germain RN, Cui M (2012) Superpenetration optical microscopy by iterative multiphoton adaptive compensation technique. *Proc Natl Acad Sci USA* 109:8434–8439.
- Tomer R, Ye L, Hsueh B, Deisseroth K (2014) Advanced CLARITY for rapid and high-resolution imaging of intact tissues. *Nat Protocols* 9:1682–1697.
- Weber M, Huisken J (2011) Light sheet microscopy for real-time developmental biology. *Curr Opin Gen Dev* 21:566–572.